Available online at www.sciencedirect.com
ScienceDirect
Proceedings of the Combustion Institute 31 (2007) 491–499
Proceedings of the Combustion Institute
www.elsevier.com/locate/proci

PAH emissions from high-temperature oxidation of vaporized anthracene

Jennifer DeCoster [a], Ali Ergut [a], Yiannis A. Levendis [a,*], Henning Richter [b], Jack B. Howard [b], Joel B. Carlson [c]

[a] *Department of Mechanical and Industrial Engineering, Northeastern University, Boston, MA 02115, USA*
[b] *Department of Chemical Engineering, Massachusetts Institute of Technology, Cambridge, MA 02139, USA*
[c] *US Army SBCCOM—Natick Soldier Center, Natick, MA 01760, USA*

Abstract

The presence of polycyclic aromatic hydrocarbons/compounds (PAH/PAC) in the exhaust of combustion equipment as well as their growth to soot particles depends on the balance of formation and depletion reaction pathways. Detailed understanding of PAH oxidation is necessary for a correct quantitative description of combustion processes. This study focuses on the high-temperature oxidation of anthracene, a 3-ring PAH, by molecular oxygen. By reacting this already formed PAH, under non-sooting conditions, its oxidative depletion processes were isolated from its formation processes, as well as from soot formation pathways. Anthracene powder, fluidized in nitrogen, was introduced into a two-stage electrically heated laminar-flow drop-tube furnace. In the first stage, kept at 900 °C, anthracene was vaporized. Thereafter, upon mixing with preheated oxygen-containing gases in a venturi, gaseous anthracene was oxidized in the second furnace at oxygen mole fractions of 1–5% and gas temperatures of 950–1050 °C. Gas temperature and velocity profiles in the furnaces, as well as anthracene particle vaporization trajectories were obtained with a computational fluid dynamics code. Sampling, followed by chemical analysis, was conducted at three locations within the oxidizing furnace. Trends with residence time show increasing CO and CO_2 yields in the furnace and gradually decreasing O_2. CO increased with higher oxidizing temperatures and oxygen concentrations. Acetylene was the most abundant light hydrocarbon, followed by methane, ethylene, benzene, propylene and ethyl acetylene. Prevalent PAC included fluorene-9-one, 9,10-anthracenodione, biphenylene, dibenzofuran, fluorene, indene, naphthalene, anthrone, xanthone and 2-naphthalenecarboxaldehyde. Most species' yields increased with rising oxidation temperatures. A global anthracene reaction rate with oxygen was deduced, and an activation energy of 71 kJ/mol was calculated. An anthracene oxidation reaction scheme was proposed.
© 2006 The Combustion Institute. Published by Elsevier Inc. All rights reserved.

Keywords: Anthracene; Oxidation; PAH; Rate constant; Reaction pathways

1. Introduction

Concentrations of polycyclic aromatic hydrocarbons (PAH) in the exhaust gases of combustors are the result of competing growth and depletion

* [redacted].

1540-7489/$ - see front matter © 2006 The Combustion Institute. Published by Elsevier Inc. All rights reserved.
doi:10.1016/j.proci.2006.07.211

processes. Depending on parameters such as equivalence ratio and temperature, depletion of PAH formed in the reaction zone can occur by subsequent oxidation [1–3] or conversion to soot [3,4]. Reactions with O, OH and O_2 are known to be important in oxidation of PAH [1–3] but the details are unclear, especially in reactions with high molecular weight PAH. Partially oxidized PAH are likely intermediates prior to decomposition to smaller hydrocarbon units and—under certain conditions—complete conversion to CO, CO_2 and H_2O. Due to the role of PAH as soot precursors, the lack of understanding of their oxidation chemistry limits the quantitative description of particulate formation. Few solid kinetic data on the gas phase oxidation of PAH are available, and in most cases the reaction pathways and even the major intermediates are unknown.

Rates of some of the elementary steps in PAH oxidation have been measured directly, but usually these are only available for the very first step in the complex reaction cascade. For example, kinetics of reactions of benzene and naphthalene with OH radicals were measured in a laser photolysis/resonance fluorescence system and the stability of the $C_{10}H_8OH$ adduct was found to be higher than that of C_6H_6OH [5], suggesting that resonant stabilization of the π-radicals formed by addition reactions may be more important for PAH than for benzene. However, no information is available on the subsequent reactions of the $C_{10}H_8OH$ adduct. Also, relative contributions of hydrogen-abstraction and direct addition oxidating species are expected to depend strongly on temperature, pressure and the size of the molecule. Reactions of biphenyl, methylnaphthalenes and phenanthrene with $O(^3P)$ were measured in a temperature range from 298 to 873 K in a low-pressure microwave discharge flow system with mass spectrometric detection [6]. Formation of phenol-type adducts was suggested to be the major reaction channel and rate constants were found to increase in the following order: benzene, biphenyl, phenanthrene, methylnaphthalenes. Reactivity of phenanthrene was similar to that of naphthalene.

Global oxidation rates of selected PAH have been recently determined in this laboratory, in the afterburner of two-stage batch-combustion of polystyrene [7]. As expected, oxidation rates increased for all species with gas temperature, but it was difficult to rationalize the observed differences in the oxidation rates of the various PAH. Nevertheless, the observed fast oxidation of fluorene suggests a correlation between molecular structure and oxidation rates, e.g., 9-fluorenone could be a plausible initial product. Indeed, 9-fluorenone and other PAH ketones have been detected mixed with PAH in diesel emissions and in the environment, and some of the PAH are known to be readily oxidized to ketones even at low temperature [8]. The most detailed study of the gas-phase oxidation of a PAH was performed by Shaddix et al. [9] who measured the stable intermediates formed in the oxidation of 1-methylnaphthalene at 1160–1200 K, in an atmospheric pressure flow reactor. They constructed a kinetic model consistent with the data [10]. Reaction pathway analysis indicated that the primary reaction was H-abstraction from the methyl side-chain, but additions of O and H atoms to the aromatic rings were also important. Reaction pathways will likely be considerably different for un-substituted PAH, which do not have any readily abstractable H atoms. Also, the chemically activated reactions that follow addition of a radical to a PAH are expected to show strong temperature dependence [11].

Anthracene, a three-ring PAH, was selected for this study because aromatics containing the anthracene configuration are known for high thermal reactivity [12,13] and propensity for soot formation [14,15]. Moreover, because of its molecular symmetry (it contains only three unique peripheral carbon positions: 9, 1, and 2) the number of possible products of thermal treatment of anthracene is limited, and this simplifies product analysis [16].

Although there has been an investigation on the products of high-temperature pyrolysis of anthracene [16], high-temperature oxidation of anthracene in particular, and PAH in general, has very little experimental history. Exploratory work on anthracene oxidation was recently conducted as a master thesis carried out at MIT by the visiting student I. Griful Millet, under the supervision of H. Richter and J.B. Howard [17]. In that work, transient (batch) oxidation of anthracene was investigated in a muffle furnace at temperatures between 500 and 800 °C, and gas compositions from 2.5 to 40% O_2 in helium. Major products identified by GC/MS were anthrone and 9,10-anthracenodione, i.e., single- and double-oxidized anthracene. Also xanthone and other oxygenated PAC formed after loss of one to three carbon units, including 2-naphthalenecarboxaldehyde, 1-*H*-phenalen-1-one, fluorene-9-one, 4-hydroxy-9-fluorenone and 1-hydroxy-9,10-anthracenodione were detected.

Herein, the exploratory work of Griful Millet [17] on batch combustion of anthracene was extended to obtain time-resolution of the intermediate species formations and products. Anthracene was pulverized, fluidized in nitrogen and introduced into a vaporizer furnace. The effluent of this furnace was then mixed with oxygen and oxidation of this premixed gaseous charge occurred in a secondary furnace. Reactions occurred therein at steady-state/steady-flow, high-temperatures and known equivalence ratios, ϕ. Oxygen mole fractions were low (1–5%), as the determination of reaction rates requires the consumption of a quantifiable amount of reactant

but without its complete depletion, otherwise the reaction time would be unknown. Low oxygen mole fractions also prevented ignition of the charge and, because of the low oxidizing temperatures, formation of soot was avoided which would have been an anthracene depletion pathway competing with the oxidation reactions. Sampling along the centerline of the furnace allowed temporal-resolution of the evolved products.

2. Experimental techniques and procedure

2.1. Experimental apparatus and conditions

Anthracene powder from *Aldrich Chemical* was crushed and sieved to 110–150 μm. Tests were conducted in a two-stage electrically heated, drop-tube furnace (*ATS Systems*) at 1 atm. The apparatus consisted of an upper furnace where the anthracene particles vaporized and a lower furnace where oxidation occurred (Fig. 1). Particles were introduced into the vaporizing furnace via a long hypodermic tube (1.1 mm i.d.; *Micro-Group*) with a vibrated glass vial coupled to a syringe pump (*Harvard Apparatus*). The tubing was vibrated to its natural frequency by two vibrators (Vibro-Graver by *Alltech*) to warrant a steady flow of anthracene particles to the vaporizing furnace, in a 2 L min^{-1} stream of nitrogen. Despite anthracene's propensity to form soot, a previous study on anthracene pyrolysis in argon reported that there was little evidence of soot (<1 wt%) at

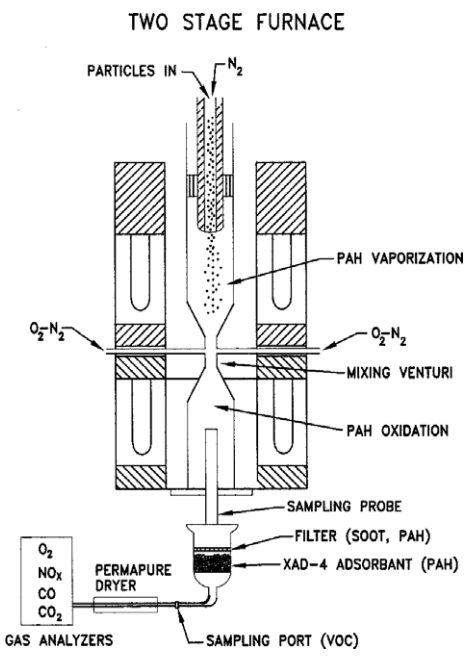

Fig. 1. Schematic of the two-stage (vaporizer + oxidizer) furnace apparatus.

$T \leqslant 927$ °C [16]. Hence, the vaporizer furnace herein was operated at 900 °C since this was the *minimum* temperature that completely vaporized the injected anthracene particles. While vaporizing anthracene particles remained at their sublimation/boiling point temperature range (226–340 °C), parcels of released vapor may have briefly heated up to higher temperatures. However, as soot was absent such temperatures must be much less than 927 °C. At $T \approx 700$ °C anthracene's decomposition has been reported to be very limited, with only a few percent pyrolyzing to bianthryls [14]. As gaseous phase anthracene in nitrogen exited this furnace, it was mixed with four radially-placed jets ejecting 3 L min^{-1} total of oxygen-nitrogen gases, preheated to 300 °C. The venturi was designed so that the radial jets reached its centerline to ensure effective mixing [19].

At the experimental gas flow rates, input oxygen concentrations of 1.2 and 5%, and the average anthracene powder flow rate of 0.34 g min^{-1} the equivalence ratios, ϕ, were 12.7 and 3, respectively. The anthracene mole fraction in the mixture was determined to be approximately 0.01 for both oxygen concentrations.

2.2. Combustion effluent sampling

The products of anthracene oxidation were sampled at three points, along the centerline of the secondary furnace, located in the heated zone at 31.8, 36.3 and 40.8 cm below the center of the venturi mixer. Gas residence times between consecutive sampling points were in the order of 0.1 s. Sampling was performed iso-axially and iso-kinetically using a 4.2 mm i.d., water-cooled stainless steel probe inserted into the oxidizer furnace via a *Cajon*™ fitting. The outer surface of the probe was insulated with layers of alumina blanket joined by alumina-based cement (*Zircar Ceramics Inc.*). The probe was attached to a sampling stage, encompassing a paper filter (*Whatman*) to capture condensed-phase PAH, and a chamber where 30 ml of XAD-4 absorbent (*Aldrich*) captured gas-phase PAH, see Fig. 1.

2.3. Sampling and detection of volatile light hydrocarbons and major fixed gases

Gas-tight glass syringes were used to sample gaseous effluent through a septum located after the XAD-4 resin stage (see Fig. 1). The collected gases were then injected into a gas chromatograph (*Agilent* GC 6890). Fixed gases (O_2, CO, and CO_2) were analyzed with a 100/120 Carbosieve S-II column, connected to a thermal conductivity detector (TCD). Light hydrocarbons were analyzed with a HP-5/Al_2O_3 30 m × 0.32 mm capillary column with a film thickness of 0.25 μm, connected to a flame ionization detector (FID). Targeted

products were quantified using calibration gas mixtures.

2.4. PAH extraction and analysis by gas chromatography—mass spectrometry

Following the oxidation experiments, the filters and XAD-4 resins were spiked with a 50 μL internal standard containing 50 μg each of naphthalene-d_8, acenaphthene-d_{10}, anthracene-d_{10}, chrysene-d_{12} and perylene-d_{12}. A *Dionex* ASE 200 Accelerated Solvent Extractor was used to extract the organic compounds from the filters and the resins together. XAD-4 resin and filter blanks as well as combustion blanks were extracted and analyzed. Details of the extraction technique are given in Ref. [18]. Identified aldehyde components were spiked onto XAD-4 resin and the recovery from XAD-4 was calculated. The responses of the aldehydes/ketones were used to develop a relative response factor (RRF), which was used to calculate the aldehyde/ketone concentration, based on the response from the appropriate internal standard.

Chemical analysis of extracts was conducted by means of gas chromatography coupled to mass spectrometry (GC–MS) using a Hewlett-Packard (HP) Model 5890 gas chromatograph equipped with a HP Model 5971 mass selective detector. Sample preparation, the operating conditions of the GC–MS system and the data reduction were described previously [11,18]. Species identification was based on the NIST and Wiley mass spectral libraries, and known retention times for isomers were used. In order to assess the reproducibility of the PAH analysis, triplicate oxidation experiments were performed. The experimental procedure was kept consistent in all evaluations to ensure the validity of comparative values and relative trends.

The extraction efficiency for the PAH species is the amount of standard recovered from the sample divided by the amount of the deuterated compounds in the internal standard solution. The National Functional Guidelines recommend a recovery of greater than 50% for the aforementioned five internal standards which was exceeded herein (59, 74, 85, 98, and 100%).

3. Results and discussion

3.1. Gas temperature measurements

Temperature profiles of the gas in the vaporizer and oxidizer furnaces were obtained along their vertical centerline using a 48 inch type-K *Omega* thermocouple, see Fig. 2. Product sampling was performed in the nearly-constant temperature region of the oxidizer furnace's heated zone,

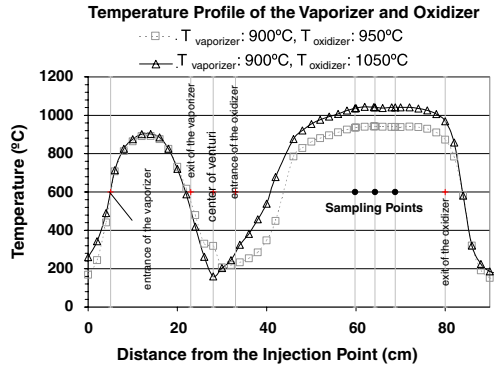

Fig. 2. Temperature profiles in vaporizer and oxidizer furnaces.

where variations of not more than ±10 K were observed.

3.2. Anthracene particle vaporization calculations/simulations

Calculations were performed in order to determine whether vaporization of the injected anthracene particles (110–150 μm) was to be expected within the heated zone of the first-stage furnace. The distance and the time that the largest diameter anthracene particles need to travel to vaporize completely were evaluated by accounting for the heat-up to the boiling temperature and for the ensuing vaporization/sublimation at constant temperature, as outlined in [19,20]. Results from these calculations were compared to computations executed with the finite-difference numerical code *Fluent* 6.0, see Fig. 3.

Both methods yielded similar particle time-of-flight outcomes, i.e., ~175 ms. There was some disagreement, however, on the prediction of particle penetration in the vaporizer furnace (8.5 vs. 11.5 cm), which may be because the calculations were conducted assuming constant gas temperature while, for computations, *Fluent* takes into

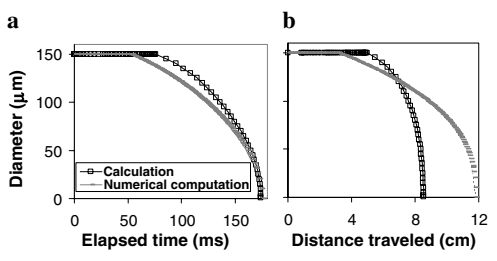

Fig. 3. Diameter of a 150 μm anthracene particle vs. (a) time to vaporize and (b) traveled distance to vaporize; results of both the numerical computations (*Fluent*) and calculations are superimposed.

account the input experimental temperature profile along the axis of the vaporizer. Nevertheless, both methods indicated that the injected anthracene particles, (110–150 μm) were expected to vaporize inside the vaporizer (upper) furnace, whose hot zone extends 19 cm from the injection point. Even so, due to the nature of this powder, clumping of particles while feeding into the injector was difficult to completely avoid.

Although ensuring vaporization of the anthracene particles was important, re-condensation at the venturi was also a concern. The partial pressure of anthracene vapors in the vaporizer furnace was calculated to be ~0.023 atm, corresponding to the vapor pressure of anthracene at ~195 °C [21]. Figure 2 shows the gas temperature dipping to this point only at the center of venturi where additional gas is mixed, decreasing the anthracene partial pressure. Hence, recondensation of anthracene at the venturi is not expected.

3.3. Emission yields

Yields of major gas products (CO, CO_2 and O_2) and light hydrocarbons, sampled inside the oxidizer furnace, are shown in Fig. 4. Yields, in mg g^{-1} of anthracene injected, of CO and CO_2 increased from 20 (1217 ppm) to 72 (4040 ppm) and from 74 (2900 ppm) to 184 (6500 ppm), respectively, at 1.2% O_2, 950 °C. Corresponding O_2 yields (mg g^{-1} of anthracene injected) decreased from 258 (1.40%) to 214 (1.05%), see Fig. 4a. At 1.2% O_2, 1050 °C, CO and CO_2 yields varied only mildly in the sampling zone, around 80 and 160 mg/g, respectively (Fig. 4b). At 5% initial O_2, the absolute values of both CO and CO_2 increased by factors of 1.5 and 2, respectively, compared to the latter case (Fig. 4c). Oxygen

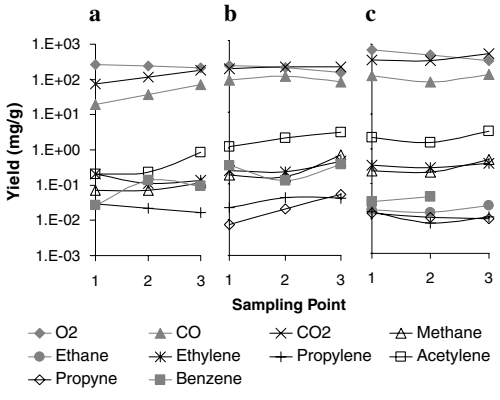

Fig. 4. Plot of fixed gas and light hydrocarbon yields (mg/g of anthracene injected). $T_{vaporizer}$ for all cases was 900 °C. (a) $T_{oxidizer}$ = 950 °C, $[O_2]$ = 1.2%; (b) $T_{oxidizer}$ = 1050 °C, $[O_2]$ = 1.2%; (c) $T_{oxidizer}$ = 1050 °C, $[O_2]$ = 5%. Δt between sampling points was ~80 ms.

was consumed faster at the higher furnace temperature, even before the first sampling point.

The most prevalent light volatile hydrocarbon was acetylene, followed by ethylene, methane, benzene and propylene, see Fig. 4. In most cases the concentration of light hydrocarbons increased along the furnace axis, especially at the lower initial oxygen concentration (1.2%), see Figs. 4a and b. Furthermore, the mole fractions of light hydrocarbons increased with furnace temperature, and at 1050 °C, propyne was also detected. As input oxygen concentration increased from 1.2 to 5%, the yields of prevalent hydrocarbons remained nearly unchanged, whereas benzene, propyne and propylene yields decreased by factors of up to 10, 5 and 6, respectively. Ethane was detected only at 5% initial O_2 case. Ethyl acetylene was detected in all tests but was not quantified.

Polycyclic aromatic compounds (PAC) were captured both in the gaseous and condensed phases. The combined PAC yields in the two phases are presented. Yields of unreacted anthracene together with other detected PAC are shown in Fig. 5. Under all experimental conditions, fluorene-9-one, 9,10-anthracenodione, biphenylene, dibenzofuran, fluorene, 1*H*-phenalene, indene, anthrone, 2-naphthalenecarboxaldehyde, acenaphthylene, phenanthrene, phenylacetylene and 4-methylphenanthrene were the most prevalent PAC. This composition of the product mixture is very similar to that detected in Millet's thesis [17]. Differences amounted to 1-hydroxy-9,10-anthracenodione which was detected therein but not herein; and to biphenylene, dibenzofuran, fluorene, indene, acenaphthylene and naphthalene, which were present in all experiments herein, but were not reported by Millet [17].

At the oxidizer temperature of 950 °C and 1.2% O_2, most PAC yields were in the range of 50–1000 μg/g of anthracene, see Fig. 5a. Major product PAC yields over 1000 μg/g of anthracene were 9,10-anthracenodione, naphthalene and fluorene-9-one.

Experiments at 1050 °C and 1.2% O_2 produced yields that were on average much higher than those at 950 °C, some components increased by a factor of five, see Fig. 5b. Biphenylene and fluorene-9-one yields increased the most, whereas 9,10-anthracenodione and 2-naphthalenecarboxaldehyde increased only slightly with rising oxidizing temperature. Biphenylene, was generated at 5000–16,000 μg/g of anthracene, followed by fluorene-9-one, naphthalene, fluorene, acenaphthylene, 9,10-anthracenodione, 1*H*-phenalene, phenanthrene, anthrone, dibenzofuran, phenylacetylene, indene, etc.

Experiments at 1050 °C and 5% O_2 produced yields that were overall comparable to those in the lower oxygen case above, see Fig. 5c. Under these conditions fluorene-9-one resulted in the highest yield (9000–16,000 μg/g of anthracene)

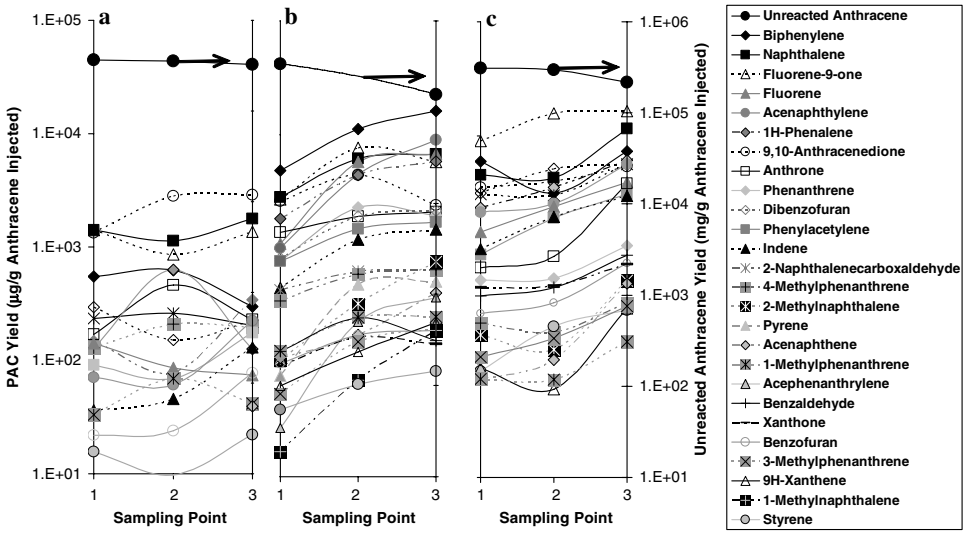

Fig. 5. Plot of PAC yields (μg/g of anthracene injected). $T_{vaporizer}$ for all cases was 900 °C. (a) $T_{oxidizer} = 950$ °C, $[O_2] = 1.2\%$; (b) $T_{oxidizer} = 1050$ °C, $[O_2]=1.2\%$; (c) $T_{oxidizer} = 1050$ °C, $[O_2] = 5\%$. Δt between sampling points was ~80 ms.

followed by biphenylene and naphthalene. Some prominent PAC byproducts such as biphenylene, fluorene, phenanthrene and acenaphthylene, decreased in yields with increasing oxygen; others, especially oxygenated ones, such as fluorene-9-one, 2-naphthalencarboxaldehyde and dibenzofuran increased significantly together with naphthalene.

Generally, but not in all cases, PAC yields increased along the centerline of the furnace, as anthracene was consumed. Moreover, some PAC were predominately detected in the gas-phase, others in the condensed-phase. For instance, in all three series of experiments, naphthalene, indene, phenylacetylene, benzaldehyde, benzofuran and styrene yields were found mostly as gaseous PAC. Biphenylene, acenaphthylene, 2-methylnaphthalene, 1-methylnaphthalene, phenanthrene and 1-methylphenanthrene were found in both phases, whereas the remaining species were found nearly entirely in the condensed phase.

3.4. Oxidation of anthracene: reaction pathways and rate

Measurement of reaction products as function of reaction time (Figs. 4 and 5) led to better insight into prevalent reactions involved in anthracene oxidation. The resulting reaction scheme, given in Fig. 6, shows formation of anthrone as a major initial oxidation product. Consistent with previous observations in combustion environments [3], isomerization to phenanthrene, which is oxidized subsequently, represents a competing pathway. Oxidation of

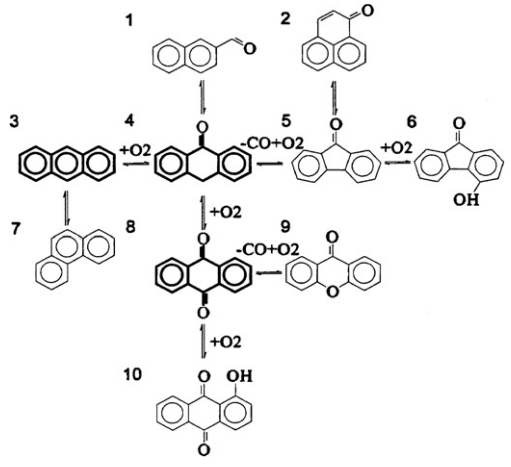

Fig. 6. Main products and proposed reaction pathways for anthracene oxidation. (1) 2-Naphthalenecarboxaldehyde, (2) 1*H*-phenalen-1-one, (3) anthracene, (4) anthrone, (5) fluorene-9-one, (6) 4-hydroxy-9-fluorenone, (7) phenanthrene, (8) 9,10-anthracenodione, (9) Xanthone, (10) 1-hydroxy-9,10-anthracenodione.

anthrone to 9,10-anthracenodione is a following reaction step. It should be noted that 9,10-anthracenodione has structural features similar to *p*-benzoquinone which has been discussed as a thermally stable intermediate of benzene oxidation [2,4]. Naphthalenecarboxaldehyde is another key intermediate of continued anthracene depletion. While elemental reactions leading to its formation still need to be identified, unimolecular CO loss yields naphthalene, another major

intermediate (Fig. 5, not shown in Fig. 6). Oxidation of naphthalene to naphthol or napthoxy, followed by another unimolecular CO loss step [3], explains the formation of indene which is abundant in the product mixtures (Fig. 5). Benzene is likely to be product of the further indene decomposition/oxidation. Its lower yields at the higher oxygen concentration of 5% is consistent with its fast subsequent oxidation. A detailed quantitative reaction mechanism describing benzene oxidation has been discussed previously [2,4] and explains semi-quantitatively the presence of acetylene, propylene, CO and CO_2 in the present work.

Well-defined experimental conditions, including good temperature control, allowed for the determination of global rate constants describing anthracene oxidation at different temperatures. Due to the excess of oxygen, leading to its depletion by not more than 25% (Fig. 4) between sampling points, anthracene oxidation was treated as a pseudo-first order chemical reaction:

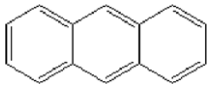

$$+ O_2 \xleftrightarrow{k} PRODUCTS$$

Rate constants were obtained for the different temperatures and oxygen partial pressures from the experiments conducted herein in the drop-tube furnace and from those of Millet [17] in the muffle furnace. Reaction rates were determined between the highest and the middle sampling points, and then again between the middle and the lowest sampling points and averages were taken. Gas temperatures along the sampling locations were assumed constant, as the profile in Fig. 2 shows variations of not more than ±10 K. Rate constants for the reactions were obtained as follows:

$$\frac{d[\text{Anthracene}]}{dt} = -k[\text{Anthracene}][O_2]$$

$[O_2]$ was assumed to be constant throughout the reaction, and was set at the average value between two sampling points, i.e., $[O_2] = \frac{[O_2]_f + [O_2]_0}{2}$. The rate constant ($k$) was obtained by integrating the above equation,

$$k = -\frac{\ln \frac{[\text{Anthracene}]_f}{[\text{Anthracene}]_0}}{[O_2]\Delta t}$$

The residence time, Δt, between the sampling points is calculated based on the integrated velocity profile at the centerline as obtained by the *Fluent* code, using the experimentally obtained gas temperature profile as input. Moreover, Roesler [22], using classical reactor theory, suggested that the chemistry in laminar flow reactors with fully developed velocity profiles follows plug flow behavior along the centerline stream on the timescale defined by the local velocity. For systems, such as the one herein, where the Damkoehler number exceeds 40, radial mass transport becomes locally negligible.

In this study, two oxidizing furnace temperatures were explored, therefore, two rate constants were calculated. The same approach was applied to 1.2 and 5% O_2 concentration cases at 1050 °C. Results are consistent with the previous work of Millet [17]. Based on both data sets depicted in Fig. 7 (from steady-state combustion in the drop-tube and from unsteady combustion in the muffle furnace), and assuming Arrhenius behavior, a rate constant of $1 \times 10^{10} \exp(-71\ \text{kJ mol}^{-1}/RT)$ was deduced, where $R = 0.008314\ \text{kJ mol}^{-1}\ \text{K}$.

Finally, it should be noted that, under most conditions, anthracene oxidation by O_2, described quantitatively by the global reactions deduced here, occurs in addition to direct oxidation by the following sequence:

$$O_2 + \text{anthracene} \rightarrow HO_2 + \text{anthracyl}$$

$$\text{anthracyl} + O_2 \rightarrow \text{products}$$

Observation of significant quantities of acephenanthrylene and fluoranthene (Fig. 5) as well as of acetylene (Fig. 4) is consistent with the formation of the aceanthrylene by addition of acetylene to 1- and 9-anthracyl radicals followed by ring closure and thermal interconversion [23]. Similarly, acenaphthylene, also observed in the present work, is formed via the reaction of 1-naphthyl radicals with acetylene.

Quantitative assessment of the relative contributions of both pathways requires sufficiently precise kinetic data describing hydrogen abstraction and anthracyl concentrations. However, compilation of a kinetic model, including this reaction sequence followed by the comparison of predicted time-dependent concentrations of anthracene and major intermediates with determination of

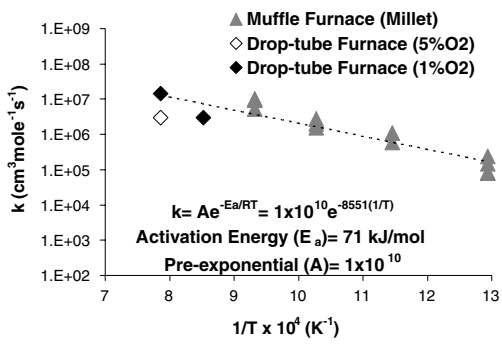

Fig. 7. Plot of the global rate constant, k vs. $1/T$ for oxidation of anthracene.

reaction fluxes, can provide additional insight. Development of such detailed model will be part of future work.

4. Conclusions

Vaporization of anthracene particles and subsequent oxidation of gas-phase anthracene took place in a two-stage laminar-flow, drop-tube furnace at fuel-rich, atmospheric conditions. The upper stage was a vaporizer furnace where anthracene particles were injected, heated and vaporized in nitrogen. This stage was followed by a venturi mixer where oxygen was introduced. The bottom stage was an oxidizer furnace where anthracene vapors oxidized at fuel-rich conditions. Sampling was conducted at three constant-temperature locations along the centerline of the oxidizer furnace. Analysis of the sampled gases was performed to assess the rate of consumption of anthracene and to identify the by-products of oxidation. Yields of CO and CO_2 showed increasing trends with time or distance traveled in the oxidizing furnace at the lower temperature, whereas they did not significantly change at the higher temperature. The average values of CO steadily increased with higher oxidizing temperatures and oxygen concentrations. On the other hand, CO_2 exhibited trends like those of CO, but were more sensitive to oxygen concentration than temperature. As the oxidizing temperature increased, more oxygen was consumed. GC–MS analysis revealed many prevalent PAC, including unreacted anthracene, fluorene-9-one, 9,10-anthracenodione, 1-H-phenalene, biphenylene, naphthalene, dibenzofuran, fluorene, acenaphthylene and anthrone. Other products resulted in lower yields.

PAC product yields increased by up to an order of magnitude when the oxidizer was operated 100 °C higher. Biphenylene and fluorene-9-one yields increased the most, whereas 9,10-anthracenodione only slightly increased with the rise in oxidizing temperature. Most major oxygenated species, such as 2-naphthalenecarboxaldehyde, dibenzofuran and fluorene-9-one, together with naphthalene, increased with oxygen concentration. The yields of other PAC with no oxygen atom in their molecules (e.g. biphenylene, fluorene, acenaphthylene, and 1*H*-phenalene) decreased. The most abundant light volatile hydrocarbons were acetylene, ethylene, methane, benzene and propylene. When operating with 1.2% oxygen concentration, benzene, propyne and propylene yields were higher than at the 5% conditions. Yields of light hydrocarbons increased with furnace temperature; acetylene yields increased, more than any other species, as temperature and oxygen concentration increased.

Based on the aforementioned detected oxidation byproducts an anthracene oxidation pathway scheme was proposed. Moreover, a global rate expression for oxidation of anthracene was deduced to be; $\ln\{[\text{Anthracene}]_f/[\text{Anthracene}]_0\} = -1 \times 10^{10}\exp(-8551/T(\text{K})) \times [\text{O}_2]_0 \times \Delta t$, at temperatures in the broad neighborhood of 1000 °C, which are pertinent to practical incinerator systems (afterburners).

Acknowledgments

The authors acknowledge technical assistance/discussions from Dr. K. Taghizadeh, Dr. W.H. Green, E.F. Plummer, C. Korber-Goncalves, J. Jordan and J. Pantalone.

References

[1] L. Dupont, A. El Bakali, J.F. Pauwels, I. DaCosta, P. Meunier, H. Richter, *Combust. Flame* 135 (2003) 171–183.
[2] H. Richter, J.B. Howard, *J. Phys. Chem.* 4 (2002) 2038–2055.
[3] H. Richter, W.J. Grieco, J.B. Howard, *Combust. Flame* 119 (1999) 1.
[4] H. Richter, J.B. Howard, *Prog. Energy Combust. Sci.* 26 (2000) 565.
[5] K. Lorenz, R. Zellner, *Phys. Chem.* 87 (1983) 629.
[6] H. Frerichs, M. Tappe, H.G. Wagner, *Proc. Combust. Inst.* 23 (1990) 21.
[7] J. Wang, G. Ferreiro, H. Richter, J.B. Howard, Y.A. Levendis, J. Carlson, *Proc. Combust. Inst.* 29 (2002) 2477.
[8] D. Schuetzle, D. Cronn, A.L. Critenden, R.J. Charlson, *Environ. Sci. Technol.* 9 (1975) 838.
[9] C.R. Shaddix, K. Brezinsky, I. Glassman, *Proc. Combust. Inst.* 24 (1992) 683.
[10] C.R. Shaddix, K. Brezinsky, I. Glassman, *Combust. Flame* 108 (1997) 139.
[11] Z. Wang, J. Wang, H. Richter, Y.A. Levendis, J.B. Howard, P. Vouros, J. Carlson, *Energy Fuels* 17 (2003) 999.
[12] E. Fitzer, K. Mueller, W. Schaefer, in: P.L. Walker (Ed.), *Chemistry and Physics of Carbon*. Marcel Decker, vol. 7, 1971, p. 239.
[13] J.J. Madison, R.M. Roberts, *Ind. Eng. Chem.* 50 (1958) 237.
[14] G.M. Badger, J.K. Donnelly, T.M. Spotswood, *Aust. J. Chem.* 17 (1964) 1147.
[15] C.R. Kinney, E. DelBel, *Ind. Eng. Chem.* 46 (1954) 548.
[16] M. Wornat, A. Sarofim, A. Lafleur, *Proc. Combust. Inst.* 24 (1992) 955.
[17] I.G. Millet, *Isomerization and Oxidation of Polycyclic Aromatic Hydrocarbons (PAH)*. Master Thesis, Universitat Ramon Llull, Barcelona (Spain), 2002.
[18] J. Wang, Y.A. Levendis, H. Richter, J.B. Howard, J. Carlson, *Environ. Sci. Technol.* 35 (2001) 3541.
[19] F. Incropera, D. DeWitt, *Introduction to Heat Transfer*, John Wiley, New York, NY, 2002, p. 242.
[20] R. Heinsohn, R. Kabel, *Sources and Control of Air Pollution*, Prentice Hall, Upper Saddle River, NJ, 1999, pp. 364–365.

[21] R.C. Weast, M.J. Astle, W.H. Beyer (Eds.), *CRC Handbook of Chemistry and Physics*, CRC Press, Inc., Boca Raton, Florida, 1984, p. D-212.

[22] J.F. Roesler, *Proc. Combust. Inst.* 27 (1998) 287.

[23] L.T. Scott, N.H. Roefols, *J. Am. Chem. Soc.* 109 (1987) 5461–5465.

Comment

Judy Wornat, Louisiana State University, USA. You report biphenylene as one of your higher yield polycyclic aromatic products. What evidence do you have that the $C_{12}H_8$ product you have assigned to be biphenylene is really biphenylene and not either the $C_{12}H_8$ 2-ethynylnaphthalene or the $C_{12}H_8$ 1-ethyny1-naphthalene? In systems that have phenylacetylene, such as I believe you have, an ethphylnaphthalene seems a more likely $C_{12}H_8$ product. Since the mass spectra of biphenylene, tethynylnaphthalene, and 2-ethynylnaphthalene are very similar, one needs to show that the two ethynylnaphthalenes can be ruled out before assuming that the $C_{12}H_8$ product observed is piphenylene. Note that a typical NIST mass spectra library, used with most GC-MS instruments, does not contain the mass spectra of the ethynylnaphthalenes, so the fact that an automated search might present a "match" with biphenylene is not sufficient substantiation of biphenylene's presence.

Reply. We currently use both the Wiley and NIST searches. Retention times were used to compare the standards of biphenylene with those of the unknowns. The retention time windows are adjusted to ensure that there is no retention time overlap for these isomers. Moreover, since over the years the analytical study involved many samples of different origins and the retention times matched (samples from other fuels tested in the same lab in the past), we are confident of the results provided in the paper.